PERGAMON

Chemical Engineering Science 58 (2003) 793–800

Chemical Engineering Science

www.elsevier.com/locate/ces

Steady-state multiplicity in bioreactors: bifurcation analysis of cybernetic models

Abhijit Namjoshi[a], Achim Kienle[b], Doraiswami Ramkrishna[a,*]

[a] *School of Chemical Engineering, Purdue University, 480 Stadium Mall Drive, West Lafayette, IN 47907, USA*
[b] *Max-Planck-Institut f"ur Dynamik komplexer technischer Systeme Sandtorstrasse 1, 39106 Magdeburg, Germany*

Abstract

Biological systems have an additional level of complexity compared to other chemical systems because of the effects of metabolic regulation, a defining feature of biosystems. Metabolic regulation in the form of control of enzyme synthesis and activity leads to non-linear behavior in bioreactors. Mathematical models that take into account these control mechanisms can be very successful in capturing the peculiarities of bioreactors such as multiple steady states and periodic phenomena. Cybernetic models model the expression and activation of enzymes by the use of cybernetic control variables and have been used to explain multiplicities in hybridoma reactors. In particular Namjoshi et al. (Biotechnol. BioEng. (2002), accepted) have been able to predict the transition from batch and fed batch to continuous culture in hybridoma experiments (Biotechnol. BioEng. 67(1) (2000) 25). The resulting multiple steady states vary widely in cell mass and waste metabolites. The model captures this multiplicity and its bifurcation analysis has revealed additional steady-state branches, three unstable and one stable. The stability of the additional steady state (steady state 4) was confirmed by dynamic simulations using fed-batch strategy prior to initiation of continuous operation. Steady state 4, in view of its close proximity to steady state 3, appears to have little practical significance. The likelihood of additional steady states that may be significantly different can, however not be ignored. Thus, it seems possible to envisage other states of metabolic activity, displaying alternative flux distributions that could lead to steady states notably different from those already determined. Calculation of the most singular point of the system herein is rendered difficult by both its size and possession of non-differentiable variables. The bifurcation analysis reveals the steady-state behavior under a range of operating conditions and can be used to plan optimum bioreactor operation.
© 2003 Elsevier Science Ltd. All rights reserved.

Keywords: Cybernetic modeling; Multiplicity; Bifurcation analysis; Mammalian bioreactors

1. Introduction

The regulation of enzyme synthesis and activity in response to environmental changes is an outstanding feature of biological systems. Consequently, the treatment of cellular reactions (catalyzed by numerous specific enzymes), which constitute metabolic networks or pathways, must necessarily take an approach at variance from that used in the analysis of conventional chemical reactions. The analysis must take due cognizance of the fact that a metabolic pathway is a complex network of chemical reactions, in which the arrows representing chemical transformation can be realized only when the specific enzyme catalyzing that step is actually available in the active state. Such regulatory processes influence biochemical reactions at least as strongly as the concentrations of the reacting components do through the governing kinetics. Metabolic activities in different pathways decide the fate of substrates fed to cells as well as growth and byproduct formation. The consequences of regulation extend from exponential growth dynamics in simple batch situations to complex nonlinear behavior in the form of steady-state multiplicity and diverse periodic states in continuous systems. Of particular interest to this paper is the hybridoma reactor of Hu, Zhou, and Europa (1998) or that of Follstad, Balcarel, Stephanopoulos, and Wang (1999). Hybridomas are mammalian cells that produce antibodies when cultured on media with glucose, glutamine and other amino acids. Hu and coworkers demonstrated that starting the reactor as a batch led to the formation of the waste metabolites: lactate, alanine and ammonia whereas a fed-batch operation with controlled glucose levels reduced this byproduct formation. Batch and fed-batch cultures, therefore when made continuous, led to steady states with very different concentrations

* Corresponding author. Tel.: +1-765-494-4066; fax: +1-765-494-0805.
E-mail address: ramkrish@ecn.purdue.edu (D. Ramkrishna).

0009-2509/03/$ - see front matter © 2003 Elsevier Science Ltd. All rights reserved.
doi:10.1016/S0009-2509(02)00609-7

of biomass and waste products. Follstad and coworkers obtained multiple steady states by step changes in the dilution rate, by starting from a state of low cell mass, reducing the dilution rate, and switching back to realize a higher biomass state.

Mathematical models that capture these non-linear biological phenomena are invaluable tools for startup and control of bioreactors. Kinetic modeling techniques that do not take into account microbial regulation are therefore at a disadvantage with regard to explaining the peculiarities of bioreactors. The cybernetic framework established by Ramkrishna and co workers (Kompala, Ramkrishna, Jansen, & Tsao, 1986; Ramkrishna, 1982) takes into account microbial regulation by the use of cybernetic "u" and "v" variables that modify enzyme synthesis and enzyme activity, respectively. Enzyme systems are hypothesized to compete optimally for resource, and different pathways can be turned on or off depending on the outcome of these competitions. Metabolic pathways are thus considered to have objective functions, which are maximized by the use of cybernetic variables. This technique derives its effectiveness from relating optimal regulatory strategies only to rates of reactions competing for cellular resources.[1] Thus, it does not demand detailed mechanistic treatment of the system and hence is ideal for modeling biosystems. Namjoshi, Hu, and Ramkrishna (2003) have employed the cybernetic framework to identify a model that explains the experiments of Hu and coworkers (1998) as well as that of Follstad et al. (1999) (qualitatively). The experimental data are first subjected to metabolic flux analysis (MFA) (Europa, Gambhir, Fu, & Hu, 2000) and the resulting flux measurements are used to abstract the network by including the important reactions. The flux values under different steady-state conditions are used to identify competitions in the cybernetic model.[2] Due to the vast complexity of biochemical pathways, the modeler should focus on fluxes rather than concentrations as one does in a chemical kinetic framework. Namjoshi et al. (2003) have shown how flux measurements can be used to formulate the cybernetic model discussed in this paper. However, a more detailed understanding of the potential consequences of cybernetic models would enhance this issue of formulation.

The focus of the current paper is to subject this model to bifurcation analysis in order to explore its capabilities over the entire range of bioreactor operation. Such analysis may reveal new features such as additional steady states or limit cycles which can then be experimentally investigated, if found desirable for reactor operation. Such analysis will also help develop control strategies that will guide the algorithms to steer the bioreactor away from undesirable steady states and direct it towards more beneficial ones. Another benefit that accrues from such a bifurcation analysis is increased insight into the behavior of complex cybernetic models, which cannot be obtained merely by dynamic simulations. Furthermore, such insights may assist in the formulation and development of cybernetic models in the future.

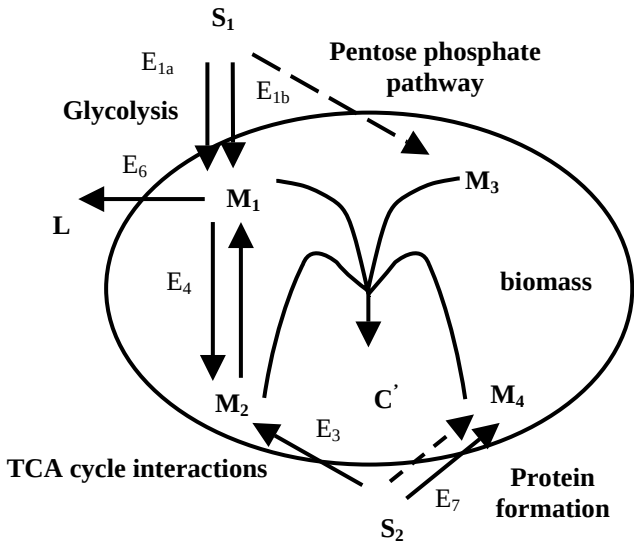

Fig. 1. Cybernetic hybridoma model schematic.

2. Cybernetic hybridoma model

We begin the discussion by a brief introduction of the cybernetic hybridoma model. Fig. 1 shows a schematic of the model, wherein the utilization of glucose (S_1) occurs via either glycolysis, catalyzed by two competing enzymes E_{1a} and E_{1b} or the pentose phosphate pathway. This leads to the formation of key intermediates pyruvate (M_1) or ribose moieties (M_3). The other nutrient glutamine (S_2) can form either the TCA intermediates, lumped as M_2 or the proteins M_4. M_1 and M_2 can interact with each other and all four intermediates M_i combine to form the rest of cell mass C'. Thus, there are multiple avenues for the production for the TCA intermediates from glucose and glutamine and regulation decides the extent to which either substrate will be used. However, glucose and glutamine still have unique contributions to cell mass and are thus called partially substitutable partially complementary nutrients. The essence of the model constitutes the substitutable competitions between enzymes: (i) E_{1a} and E_{1b}, (ii) E_3 and E_7, and (iii) E_3 and E_4, the result of which leads to multiple steady states as explained later. Also, enzyme E_6 is expressed and activated in conjunction with E_{1a} and this accounts for the coordinated biological activity of the coenzymes NAD and NADH between glycolysis and lactate formation. The model equations are detailed in

[1] The cybernetic variables u and v for reactions 1 and 2 competing in a substitutable process are calculated as $u_1 = r_1/(r_1 + r_2), u_2 = r_2/(r_1 + r_2); v_1 = r_1/\max(r_1, r_2), v_2 = r_2/\max(r_1, r_2)$.

[2] Curiously, although the MFA is used to formulate the cybernetic model by enunciating suitable optimal goals, the model itself has a viewpoint at variance from that used to carry out MFA! Thus, flux distributions predicted by the cybernetic model will only be in qualitative agreement with MFA estimates.

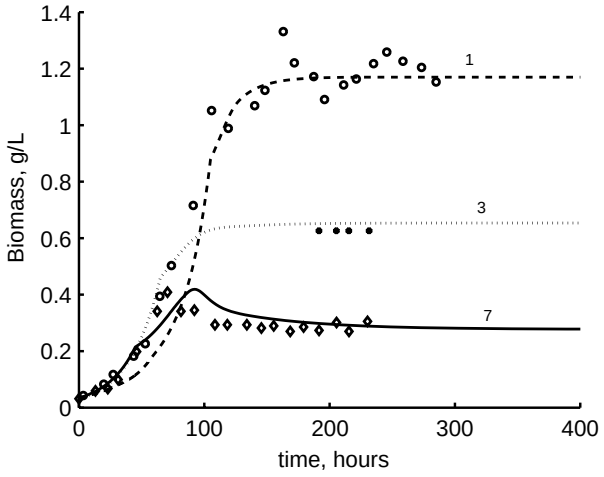

Fig. 2. Dynamics simulations of the cybernetic hybridoma model and experimental data.

Appendix A. The parameters are so identified that E_{1a} is the preferred enzyme when the glucose concentration is high, (say a batch), whereas E_{1b} dominates under glucose starvation. Similarly E_3 dominates under abundance of glutamine and E_7 wins under glutamine starvation. Thus, large concentrations of glucose and glutamine activate less efficient pathways for cell mass and subsequently antibody production (not modeled separately). A model simulation for the cell mass is shown in Fig. 2. The model successfully predicts the evolution of batch and fed-batch cultures to continuous cultures with different biomass and lactate concentrations. The diamonds denote experimental data of batch simulations, whereas the open circles denote a fed-batch simulation with glucose controlled to very low levels. The intermediate state denoted by asterisks is achieved by imperfect control of glucose in a fed-batch system. Thus, the low cell mass steady-state results from the cybernetic variable u^c_{1a} winning over u^c_{1b} and u^d_3 winning over u^d_7. The high cell mass steady state is exactly the reverse, with the intermediate steady state resulting from u^c_{1a} still dominating u^c_{1b} but u^d_3 losing to u^d_7.

3. Bifurcation analysis

The bifurcation analysis of cybernetic models is complicated by the non-differentiability of the cybernetic v variables, which contain max functions. Namjoshi and Ramkrishna (2001) addressed this problem for the models of Kompala et al. (1986) and Ramakrishna, Konopka, and Ramkrishna (1996) by considering different combinatorial cases in which the appropriate differential counterparts could approximate the v variables. Methods of continuation could then be used within the individual regimes to follow the steady states and generate the bifurcation diagrams. The meeting points of different regions manifest as sharpnesses in the curve that depict the non-differentiability of the system. On the other hand, Zhang and Henson (2001) use the commercial software AUTO to simulate the cybernetic hybridoma model of Guardia, Gambhir, Europa, Ramkrishna, and Hu (2000). This paper combines both approaches. Thus, one can use commercial software, but at the same time program it to watch for sharp corners or turning points. In the current work, dynamic simulations (Namjoshi et al., 2003) were used to generate the steady states, which were then "continued" in AUTO'97 as well as DIVA (Doedel, Wang, & Fairgrieve, 1986; Mangold, Kienle, Gilles, & Mohl, 2000) to generate bifurcation diagrams. Bifurcation diagrams are steady-state plots of state variables against a key operation parameter such as the dilution rate. The dilution rate D is one bifurcation parameter, while the fraction of glucose in the feed (γ) is the other one used explore the operating space completely.

4. Results and discussion

The types of solutions can be classified broadly as trivial and non-trivial solutions. The trivial solutions correspond to washout conditions, wherein biomass and lactate are zero and substrates correspond to feed concentrations. However, since the internal variables (intermediates and enzymes) are written as fractions of the cell mass, the internal variables are non-zero in these solutions. Thus the trivial solution values for internal variables can be thought of as the levels of these intermediates in cells about to get washed out from a continuous culture. The non-trivial solutions comprise situations in which the cells consume one or more substrates. Since only a sub-system needs to be solved (numerically) for the trivial solutions, they present another avenue to get at the non-trivial solution branches, apart from the dynamic simulations approach already discussed. In fact, one of the approaches tried here was to simulate the system at high dilution rates for different combinatorial cases. This results in different trivial solutions, which can then be subject to continuation to simulate the non-trivial solution states. One can thus classify bifurcations into two types: (i) primary bifurcations, which are (transcritical) between trivial and non-trivial solution branches, and (ii) secondary bifurcations, which arise among the non-trivial branches.

Fig. 3 shows the bifurcation diagram of biomass as a function of the dilution rate. The vertical dotted line denotes the experimental dilution rate of 0.033/h wherein the system displays up to seven non-trivial solutions in addition to three trivial ones. The trivial solution values are independent of the dilution rate and are shown as horizontal dashed lines, irrespective of their stability (Fig. 7). The approach presented here does not preclude the existence of isola or other solution branches, but they seem unlikely based on extensive numerical simulations. The non-trivial states are denoted 1–7 in decreasing order of cell mass. Of these states 1, 3 and 7 are stable (thick lines), the rest being unstable (dashed lines). The primary bifurcations seem to arise at high dilution rates, and in Fig. 3, they are simply represented by the

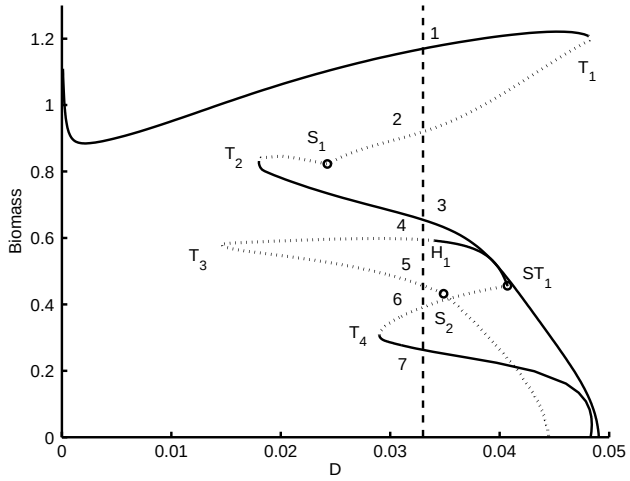

Fig. 3. Biomass concentration versus dilution rate for $\gamma = 0.693$.

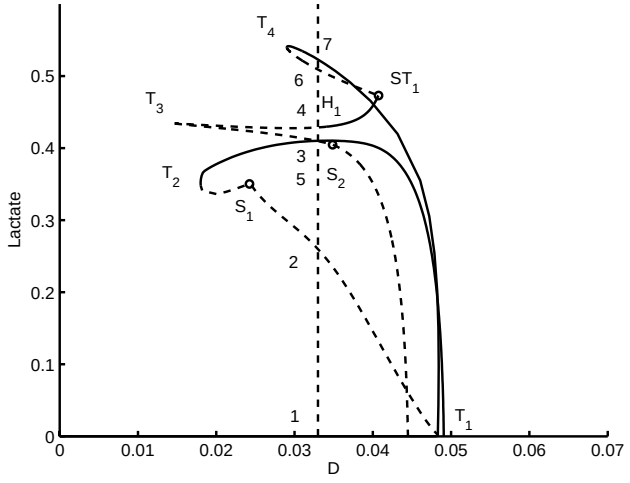

Fig. 4. Lactate concentration versus dilution rate for $\gamma = 0.693$.

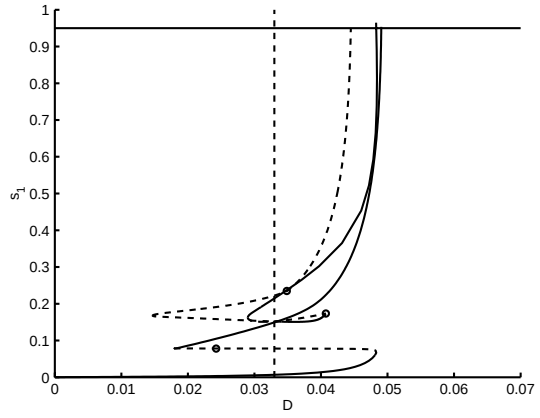

Fig. 5. Substrate s_1 concentration versus dilution rate for $\gamma = 0.693$.

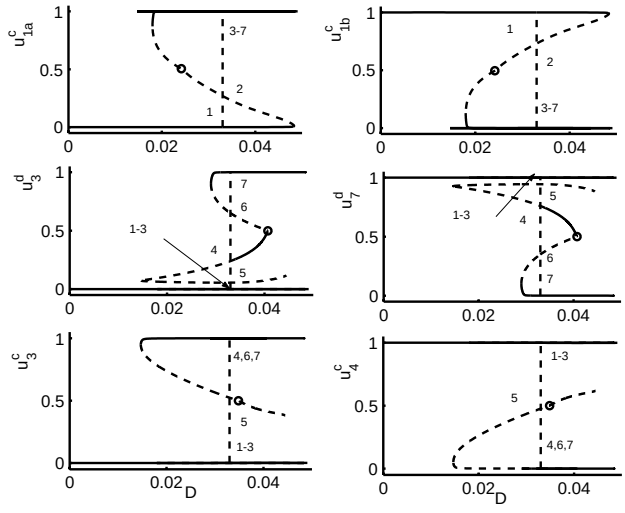

Fig. 6. Cybernetic variables versus dilution rate for $\gamma = 0.693$.

biomass and lactate levels (Fig. 4) going to zero, corroborated by the substrates reaching their feed concentrations (Fig. 5). Steady state 1 shows complete domination of u^c_{1b} over u^c_{1a} as well as that of u^d_7 over u^d_3 (Fig. 6). This means that $u^c_{1b} = 1$ and $u^c_{1a} = 0$, and enzyme E_{1b} is expressed to the maximum possible extent (dictated by the concentrations of the substrates alone) at the expense of E_{1a}. Thus, the competition has an outright winner in E_{1b}. As the dilution rate is increased, the substrate S_1 concentration slowly increases, until it reaches a point where u^c_{1a} starts picking up at the expense of u^c_{1b}. The system undergoes a turning point bifurcation (T_1) at this point resulting in a loss of stability. As we move along the unstable branch (state 2), with decrease in the dilution rate, the values of u^c_{1a} and u^c_{1b} become equal (to 0.5) at point S_1, which is a sharp corner. Further decrease in the dilution rate leads to another turning point (T_2) with a gain in stability. At this point u^c_{1a} has almost completely dominated u^c_{1b}. Further increase in dilution rate results in state 3 before the stable state eventually washes out to yield stability to a trivial solution branch. All this while, u^d_7 continues to dominate u^d_3 for the entire branches corresponding to states 1–3. This however changes for steady states 4–7 where there is not so complete a domination by u^d_7. Focus now on solution 4. This branch is unstable at the operating point, but this is as a result of a Hopf bifurcation (not shown) that occurs at point H_1. Thus, at dilution rates beyond point H_1 this branch is stable, but loses its stability as a Hopf bifurcation occurs. Interestingly, the Hopf bifurcation is also unstable, and dynamic simulations demonstrate that an initial condition 4 when simulated, results in oscillations of increasing magnitude (unstable) culminating in steady state 3 at $D = 0.033$/h. The unstable branch 4 undergoes a turning point bifurcation (T_3) at lower dilution rates, but remains unstable, resulting in solution 5. Instances of such bifurcations can also be found in the work of Uppal, Ray, and Poore (1974). The stable part of the branch

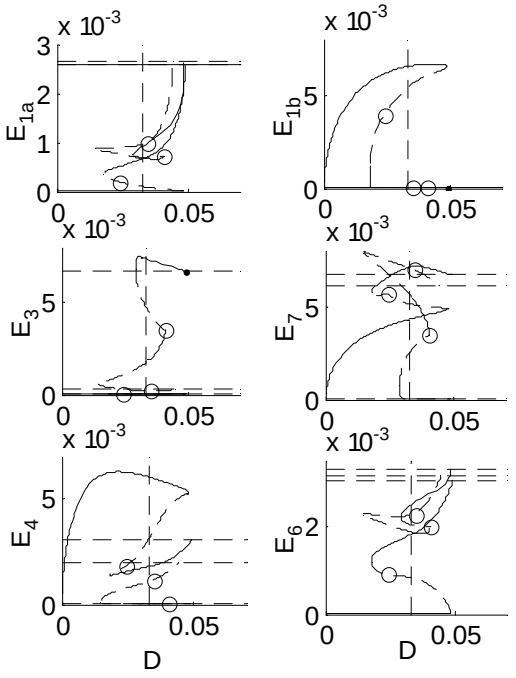

Fig. 7. Enzyme concentrations versus dilution rate for $\gamma = 0.693$.

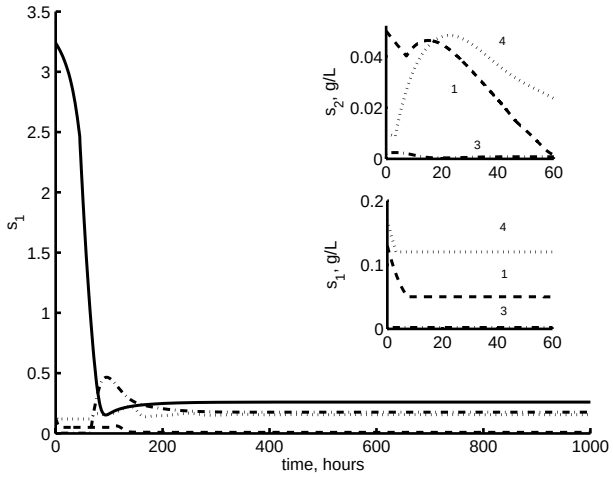

Fig. 8. Transients of glucose concentrations for $D = 0.036$/h for different start-up conditions.

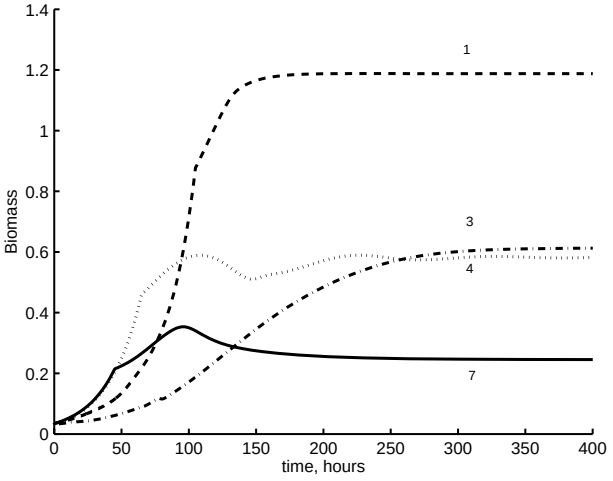

Fig. 9. Transients of biomass concentrations for $D = 0.036$/h for different start-up conditions.

with solution 4 undergoes a sharp turning point at higher dilution rates, which coincides with a sharp corner (ST_1) resulting in a loss of stability, leading to branch with solution 6. This sharp turning point is a result of the tug of war between u_3^d and u_7^d reaching a point of equal strengths. Branch 5 at higher dilution rates leads to a sharp corner before washout, this one however results from u_3^c and u_4^c reaching equal levels. Solution 6 undergoes another turning point (T_4) at decreasing dilution rates leading to a gain of stability for solution 7, which also washes out at higher dilution rates. The enzymes are depicted in Fig. 7 and the enzyme balances show some parallels with their control variables viz. the cybernetic u variables shown. The model has thus predicted an additional stable steady state (4) at dilution rates slightly higher than the experimental dilution rates.

In order to further investigate this steady state, batch and fed-batch simulations (Figs. 8, 9) similar to the experiments (Fig. 2) were performed at a dilution rate of 0.036/h, which renders state 4 to be stable. One observes that whereas the batch simulation leads to steady state of type 7 as before, fed-batch simulations lead to interesting effects. Steady state 1 results from low levels of S_1 as well as S_2 maintained in the fed batch as also in the transition to continuous mode. However steady state 4 results when the level of glutamine is relatively (compared to 3) high in the fed batch thereby leading to incomplete domination of reaction 3 by reaction 7, indicated by $u_3^d > 0$ for steady state 4. However, lower level of S_2 maintained in the fed batch leads to steady state of type 3. At a dilution rate of 0.033/h, however steady state 4 is unstable and fed batch that produced steady state 4 at $D = 0.036$/h produces steady state 3 instead. Note also that steady state 4 has an oscillatory convergence as against state 3. Although the steady states 3 and 4 are remarkably similar to each other in terms of the concentrations of external variables such as substrates and cell mass, they are different in terms of the cybernetic variable u_3^d and whereas one shows a non-oscillatory decay, the other one shows periodic behavior. Such states can pose problems for a controller that relies only on the measurements of substrates and cell mass. However, this analysis establishes the nature of such steady states and can guide the controller in steering the reactor away from these regions. States 3 and 4 also establish beyond doubt that non-linear analysis has the potential to unearth new steady states with different metabolic states than those observed experimentally.

In order to truly demonstrate the power of non-linear analysis, steady states were generated for a variety of feed

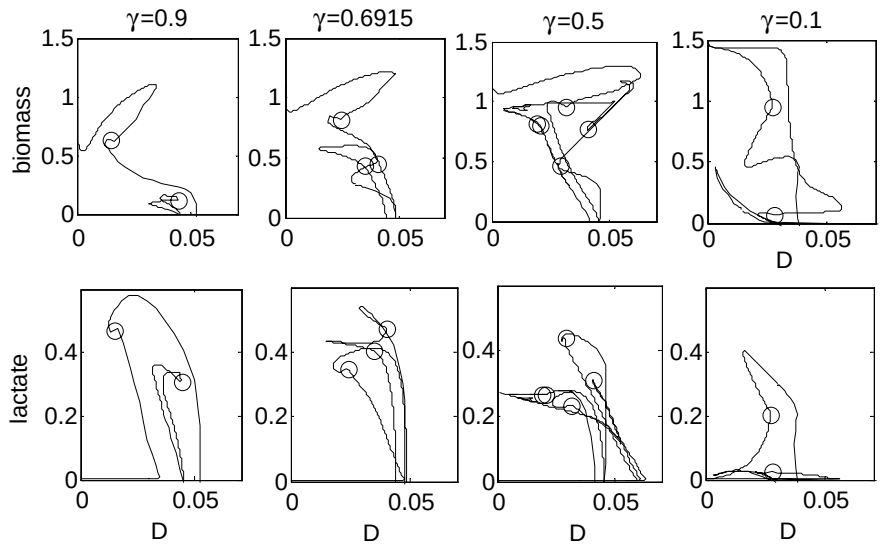

Fig. 10. Biomass and lactate concentrations versus dilution rate for a range of γ values.

substrate fractions of glucose (γ), with γ=0.693 denoting the experimental setup of Europa et al. (2000). Fig. 10 shows the bifurcation diagrams for glucose and lactate for a range of γ values. These plots also show additional structures appearing at $\gamma = 0.5$, mainly due to additional turning point bifurcations. These however do not lead to any steady states that are remarkably different in the concentrations of the external variables. Although these multidimensional plots are not easy to interpret from two-dimensional projections, it can be clearly seen that the concentration of lactate is a strong function of γ in that under low values of γ, there is very little lactate production in the different steady states. This tells us that most of the lactate is produced from glucose, which is present in low concentrations in the feed at low γ. Also, the most desirable steady state 1 corresponding to the highest cell concentration has the widest range of stability for intermediate γ values corresponding to a mixed feed scenario as against low or high γ. This confirms that the model indeed captures the partially substitutable partially complementary nature of glucose and glutamine.

Thus the model predicts the existence of multiple non-trivial solutions at medium to high dilution rates, but a unique non-trivial solution at low dilution rates. This is probably because the low substrate concentrations at low dilution rates allow unique winners of competitions between the enzyme systems that consume them. This gives us invaluable insight as to why the model predicts the transition from state 7 to state 1 when the dilution rate is decreased first and increased subsequently (Namjoshi et al., 2003), which was the experimental observation of Follstad et al. (1999). The beauty of steady-state analysis lies in its facility to plan experiments that will allow operation at the most desirable steady state. This model, for instance is built on the batch and fed-batch start-up experiments of Europa et al. (2000), but is successful in explaining at least qualitatively the experiments of Follstad (1999), a fact clearly brought about by the bifurcation analysis in this work.

5. Conclusion

The non-linear analysis of the cybernetic hybridoma model provides insight into the global steady-state behavior of the model under the conditions examined, and reveals interesting bifurcation phenomena. In the current investigation, it has unearthed the existence of an additional stable steady-state that did not arise either in the work of Europa et al. (2000) or Namjoshi et al. (2003). The steady state multiplicity observed here clearly arises from the role of metabolic regulation. The extent of its manifestation is dependent on the ability to institute initial states of the reactor both with respect to the environmental variables and the internal state of biomass. Larger cybernetic models obviously will produce increasing multiplicity of steady states that may be sampled by the system only if it can assume suitably sensitive initial conditions. It is apparent that the cybernetic approach to modeling biological reactors can lead to a plethora of non-linear behavior that has been the hallmark of chemical reaction engineering. This is not only interesting from a theoretical viewpoint but also very significant in the understanding of the role of metabolic regulation in determining the course of metabolic function.

Acknowledgements

The authors would like to thank the National Science Foundation (Grant No. 9818054-CTS) for supporting this work.

Appendix A.

Model equations for the cybernetic hybridoma model are presented below.

State variables

$$x = [\underline{x}_e^{\mathrm{T}} \quad x\ \underline{x}_i^{\mathrm{T}} \quad \underline{e}^{\mathrm{T}}]^{\mathrm{T}} \quad \text{where } \underline{x}_e^{\mathrm{T}} = [s_1 \quad s_2 \quad L],$$

$$x = \text{biomass}, \quad \underline{x}_i^{\mathrm{T}} = [m_1 \quad m_2 \quad m_3 \quad m_4\ C'],$$

$$\underline{e}^{\mathrm{T}} = [e_{1a} \quad e_{1b} \quad e_3 \quad e_4 \quad e_6 \quad e_7].$$

Kinetic vectors

$$\underline{r}^{\mathrm{T}} = [r_{1a} \quad r_{1b} \quad r_2^m \quad r_3 \quad r_4 \quad r_5 \quad r_6 \quad r_7 \quad r_7^m \quad \hat{r}_g],$$

$$\underline{r}_e^{\mathrm{T}} = [r_{e1a} \quad r_{e1b} \quad r_{e3} \quad r_{e4} \quad r_{e6} \quad r_{e7}],$$

$$\underline{r}_e^{*T} = [r_{e1a}^* \quad r_{e1b}^* \quad r_{e3}^* \quad r_{e4}^* \quad r_{e6}^* \quad r_{e7}^*],$$

$$\underline{u}^{\mathrm{T}} = [u_{1a}^c \quad u_{1b}^c\ (u_3^c\ u_3^d) u_4^c \quad u_6 \quad u_7^d],$$

$$\underline{v}^{\mathrm{T}} = [v_{1a}^c \quad v_{1b}^c \quad 1(v_3^c v_3^d) \quad v_4^c \quad 1\ v_6 \quad v_7^d \quad 1].$$

Feed concentrations

$$\underline{x}_e^{f\mathrm{T}} = [s_1^f \quad s_2^f \quad 0].$$

Dynamic equations

$$\frac{\mathrm{d}\underline{x}_e}{\mathrm{d}t} = M_e\,\mathrm{diag}(\underline{v})\underline{r}x + D(\underline{x}_e^f - \underline{x}_e),$$

$$\frac{\mathrm{d}\underline{x}_i}{\mathrm{d}t} = M_i\,\mathrm{diag}(\underline{v})\underline{r} - r_g\underline{x}_i,$$

$$\frac{\mathrm{d}\underline{e}}{\mathrm{d}t} = \underline{r}_e^* + \mathrm{diag}(\underline{r}_e)\underline{u} - (r_g + \beta)\underline{e}_i,$$

where

$$M_e = \begin{bmatrix} -1 & -1 & -1 & 0 & 0 & 0 & 0 & 0 & 0 & 0 \\ 0 & 0 & 0 & -1 & 0 & 0 & 0 & -1 & -1 & 0 \\ 0 & 0 & 0 & 0 & 0 & 0 & Y_6 & 0 & 0 & 0 \end{bmatrix},$$

$$M_i = \begin{bmatrix} Y_1 & Y_1 & 0 & 0 & -1 & Y_5 & -1 & 0 & 0 & -Y_{cm1} \\ 0 & 0 & 0 & Y_3 & Y_4 & -1 & 0 & 0 & 0 & -Y_{cm2} \\ 0 & 0 & Y_2 & 0 & 0 & 0 & 0 & 0 & 0 & -Y_{cm3} \\ 0 & 0 & 0 & 0 & 0 & 0 & 0 & Y_7 & Y_7 & -Y_{cm4} \\ 0 & 0 & 0 & 0 & 0 & 0 & 0 & 0 & 0 & 1 \end{bmatrix}.$$

Cybernetic variables

$$u_6 = u_{1a}^c = \frac{r_{1a}}{r_{1a} + r_{1b}}; \quad u_{1b}^c = \frac{r_{1b}}{r_{1a} + r_{1b}};$$

$$v_6 = v_{1a}^c = \frac{r_{1a}}{\max(r_{1a}, r_{1b})}; \quad v_{1b}^c = \frac{r_{1b}}{\max(r_{1a}, r_{1b})};$$

$$u_3^d = \frac{r_3}{r_3 + r_7}; \quad u_7^d = \frac{r_7}{r_3 + r_7};$$

$$v_3^d = \frac{r_3}{\max(r_3, r_7)}; \quad v_7^d = \frac{r_7}{\max(r_3, r_7)};$$

$$u_3^c = \frac{Y_3 r_3}{Y_3 r_3 + Y_4 r_4}; \quad u_3^c = \frac{Y_4 r_4}{Y_3 r_3 + Y_4 r_4};$$

$$v_3^c = \frac{Y_4 r_4}{\max(Y_3 r_3, Y_3 r_3)}; \quad v_4^c = \frac{Y_4 r_4}{\max(Y_3 r_3, Y_4 r_4)}.$$

Kinetic expressions

$$r_i = r_i^{\max}\left(\frac{p_i}{k_i + p_i + \dfrac{p_i^2}{K_i}}\right)\left(\frac{c'}{c' + k_g'}\right)\left(\frac{e_i}{e^{\max}}\right)$$

$$\forall i = 1a, 1b, 3, 7,$$

$$r_i = r_i^{\max}\left(\frac{p_i}{k_i + p_i}\right)\left(\frac{c'}{c' + k_g'}\right)\left(\frac{e_i}{e^{\max}}\right) \quad \forall i = 4, 6,$$

$$r_5 = r_5^{\max}\left(\frac{p_i}{k_5 + p_i}\right)\left(\frac{c'}{c' + k_g'}\right),$$

$$r_i^m = r_{im}^{\max}\left(\frac{p_i}{k_i^m + p_i}\right)\left(\frac{c'}{c' + k_g'}\right) \quad \forall i = 2, 7$$

$$r_{ei} = r_e^{\max}\left(\frac{p_i}{k_{ei} + p_i}\right) \quad \forall i = 1a, 1b, 3, 4, 6, 7,$$

$$\hat{r}_g = \prod_{i=1}^{4} \frac{m_i}{k_g + m_i};$$

$$r_g = Y_1(r_{1a}v_{1a} + r_{1b}v_{1b}) + Y_2 r_2^m + Y_3 r_3 v_3^c v_3^d + Y_7(r_7 v_7^d + r_7^m) + (Y_5 - 1)r_5 + (Y_4 - 1)r_4 v_4^c - r_6 v_6 + \hat{r}_g/1 - Y_{cm1} - Y_{cm2} - Y_{cm3} - Y_{cm4}$$

where $p_i = s_1$ for $i = 1a, 1b, 2$; s_2 for $i = 3, 7$; m_1 for $i = 4, 6$; m_2 for $i = 5$ and $v_6 = v_{1a}^c$.

The model parameters are detailed in Namjoshi et al. (2003).

References

Doedel, E., Wang, X., & Fairgrieve, T. (1986). AUTO: *Software for continuation and bifurcation problems in ordinary differential equations*. Technical Report, California Institute of Technology.

Europa, E. F., Gambhir, A., Fu, P.-C., & Hu, W.-S. (2000). Multiple steady states with distinct cellular metabolism in continuous culture of mammalian cells. *Biotechnology and Bioengineering*, *67*(1), 25–34.

Follstad, B. D., Balcarel, R. R., Stephanopoulos, G., & Wang, D. (1999). Metabolic flux analysis of hybridoma continuous culture steady state multiplicity. *Biotechnology and Bioengineering*, *63*, 675–683.

Guardia, M. J., Gambhir, A., Europa, A., Ramkrishna, D., & Hu, W.-S. (2000). Cybernetic modeling and regulation of metabolic pathways in multiple steady states of hybridoma cells. *Biotechnology Progress*, *16*, 847–853.

Hu, W.-S., Zhou, W., & Europa, L. F. (1998). Controlling mammalian cell metabolism in bioreactors. *Journal of Microbiology Biotechnology*, *8*, 8–13.

Kompala, D. S., Ramkrishna, D., Jansen, N. B., & Tsao, G. T. (1986). Investigation of bacterial growth on mixed substrates. Experimental evaluation of cybernetic models. *Biotechnology and Bioengineering*, *28*, 1044–1056.

Mangold, M., Kienle, A., Gilles, E. D., & Mohl, K. D. (2000). Nonlinear computation in DIVA—methods and applications. *Chemical Engineering Science*, *55*(2), 441–454.

Namjoshi, A. A., Hu, W.-S., & Ramkrishna, D. (2003). Unveiling steady state multiplicity in hybridoma cultures: The cybernetic approach. *Biotechnology and Bioengineering*, *81*(1), 80–91.

Namjoshi, A., & Ramkrishna, D. (2001). Multiplicity and stability of steady states in continuous bioreactors. Dissection of cybernetic models. *Chemical Engineering Science*, *56*, 5593–5607.

Ramkrishna, D. (1982). A cybernetic perspective of microbial growth. In *Foundations of biochemical engineering*: *Kinetics and thermodynamics in biological systems* Washington, DC: American Chemical Society. Editors: E. Papoutsakis, G.N. Stephanopoulos and H. Blanch.

Ramakrishna, R., Konopka, A., & Ramkrishna, D. (1996). Cybernetic modeling of growth in mixed, substitutable substrate environments. Preferential and simultaneous utilization. *Biotechnology and Bioengineering*, *52*, 141–151.

Uppal, A., Ray, W. H., & Poore, A. B. (1974). On the dynamic behavior of continuous stirred tank reactors. *Chemical Engineering Science*, *29*, 967–985.

Zhang, Y., & Henson, M. A. (2001). Bifurcation analysis of continuous biochemical reactor models. *Biotechnology Progress*, *17*, 647–660.